Time delay and the effect of the finite speed of light in atom gravimeters

Yu-Jie Tan, Cheng-Gang Shao,* and Zhong-Kun Hu†

MOE Key Laboratory of Fundamental Physical Quantities Measurement, Hubei Key Laboratory of Gravitation and Quantum Physics, School of Physics, Huazhong University of Science and Technology, Wuhan 430074, People's Republic of China

(Received 21 May 2017; published 2 August 2017)

The propagation time delay due to the finite speed of light (FSL) in atom gravimeters introduces a bias in the gravity measurement, as well as that in classical free-falling corner-cube gravimeters, which is usually termed the FSL effect. For a typical atom gravimeter, the FSL time delay is about several nanoseconds, resulting in the FSL effect, a non-negligible bias in the gravity-acceleration measurement. However, a time delay of about several microseconds, achieved by controlling the Raman-pulse timing directly, contributes a negligible effect. This interesting phenomenon motivates us to make clear two questions: first, what are the origins of the FSL effect in atom gravimeters, and second, what is the difference between the two time delays? Our analysis shows that the FSL effect in atom gravimeters is not just a matter of FSL time delay to a great extent but also the change in the effective wave vector; moreover, the FSL time delay can be quantitatively regarded as the same as the pulse time delay since both actually affect the gravity measurement by changing the two interferometer pulse separations.

DOI: 10.1103/PhysRevA.96.023604

I. INTRODUCTION

The propagation time delay due to the finite speed of light (FSL) introduces a bias in the g measurement in classical free-falling corner-cube gravimeters [1–8]. A similar effect also exists in atom gravimeters which is usually termed the FSL effect. To evaluate the performance of high-precision atom absolute gravimeters [9–14], systematic errors such as the FSL effect need to be carefully considered since they are at the level of instrument precision of the atom gravimeters developing rapidly, introducing a non-negligible bias in the g measurement. In the past few years, a few studies [15–21] discussed the FSL effect in atom gravimeters: Peters *et al.* [15,16] and Cheng *et al.* [17] considered the FSL correction introduced by the change in the effective wave vector of Raman pulses during the frequency-chirp process, Dimopoulos *et al.* [18,19] analyzed the FSL correction resulting from the time delay due to the propagation of light, and we presented [20,21] the FSL correction related to the coupling between the time delay and the change in the effective wave vector. The above results can be well summed up by [20]

$$g_{\text{measured}} = -\frac{\vec{k}_0\cdot\vec{g}}{|\vec{k}_0|}\left[1+\frac{3\vec{v}_\pi\cdot\vec{n}_1}{c}-\frac{\alpha_1-\alpha_2}{\vec{k}_0\cdot\vec{g}}\frac{2\vec{v}_\pi\cdot\vec{n}_1}{c} + \frac{\alpha_1\vec{n}_1-\alpha_2\vec{n}_2}{\vec{k}_0\cdot\vec{g}}\cdot\frac{2\vec{v}_\pi}{c}\right], \tag{1}$$

with $\vec{k}_0$ being the effective wave vector of the Raman beams at the π pulse, $\vec{v}_\pi$ being the velocity of atoms at the π pulse, c being the speed of light, and (α_1,α_2) and $(\vec{n}_1,\vec{n}_2)$ being the frequency chirps and directions of the two Raman beams, respectively. To make the FSL effect well understood, we further study this effect in this paper and attempt to make some key issues related to the FSL effect clear.

Generally speaking, the FSL effect in atom gravimeters arises from the FSL time delay. Similar to the pulse time delay achieved by controlling the Raman-pulse timing directly, the FSL time delay also changes the interferometer pulse separations and further contributes a correction to the gravity measurement. Therefore, with the same influencing mechanism, if the two time delays are equal, they should theoretically present equal corrections to the g measurement. For a typical 20-cm-long atom gravimeter, in which the velocity of atoms at the π pulse is about 0.06 m/s, the FSL time delay is about several nanoseconds, introducing the FSL effect, a bias of about 0.4 μGal in the g measurement; however, a pulse time delay of several microseconds has a negligible effect. This is an interesting phenomenon, which motivates us to make clear what the FSL effect and the difference between the FSL time delay and pulse time delay are.

The outline of this paper is as follows: in Sec. II, we show the space-time diagram of an atom gravimeter with the FSL time delay and the pulse time delay. In Sec. III, with the frequently used continuous chirp of Raman pulses, we calculate phase shifts introduced by the FSL effect and the pulse time delay, where the detuning for Raman pulses is also considered. Here, we make clear what results in the FSL effect in atom gravimeters and what the difference between the two time delays is. In Sec. IV, we present a simple discussion of the stepped-chirp mode (that is, the continuous chirp is approximated by switching between three fixed frequencies) and find this chirp mode may have the advantage of enlarging the effect of the pulse time delay in the g measurement, which has been verified experimentally [15,16]. Finally, the paper is concluded in Sec. V.

II. SPACE-TIME DIAGRAM OF AN ATOM GRAVIMETER WITH A PULSE TIME DELAY AND A FSL TIME DELAY

High-sensitivity atom interferometry plays a significant role in many precision-measurement experiments [22–29], on the basis of which atom gravimeters are being developed rapidly. The work principle of atom gravimeters based on

*cgshao@mail.hust.edu.cn
†zkhu@hust.edu.cn

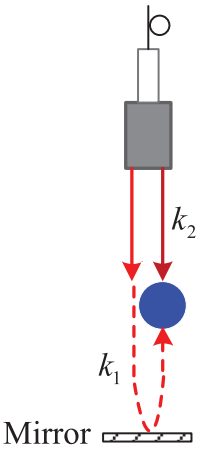

FIG. 1. A schematic of the interaction between atoms and Raman beams, with the "control light" reflected by a mirror oriented upward. The blue dot represents atoms.

two-photon stimulated Raman transitions can be described as follows [30]: it measures g with an interferometer in which atoms follow free-fall trajectories. In the measurement process, a $\pi/2$-π-$\pi/2$ Raman-pulse sequence is usually applied to coherently split, reflect, and combine the atomic wave packet and, finally, produce the interference. Then, one can obtain the gravity acceleration from the interference signal.

Figure 1 is a typical schematic describing the interaction between atoms and Raman pulses. Two laser beams with respective wave numbers k_1 and k_2 start from the top of the experimental setup; then the two counterpropagating lights, the k_2 beam and the reflected k_1 beam, form the Raman pulse. Note that due to the FSL, the $\vec{k}_1$ beam reflected by the retroreflecting mirror will reach atoms with a delay compared with the $\vec{k}_2$ beam. As the stimulated Raman transitions occur only when the two Raman beams interact with atoms simultaneously, the $\vec{k}_2$ beam can be considered a "background light," and the $\vec{k}_1$ beam can be considered a "control light," determining the change in the atom's internal state. Therefore, we can simplify the model of atom gravimeters as the control light tracking the atoms, described by Fig. 2. Assume that the directions of the control light, the $\vec{k}_1$ beam, and the $\vec{k}_2$ beam in atom gravimeters are respectively denoted by unit vectors $\vec{e}_c$, $\vec{n}_1$, and $\vec{n}_2$. In the configuration shown in Fig. 1, the control light is upward, $\vec{e}_c = \vec{n}_1$. Actually, the orientation of the control light can be adjusted upward or downward, depending on whether the mirror is set at the bottom or top of the experimental setup.

Like for classical gravimeters that monitor the position of a freely falling retroreflector using laser interferometers, we

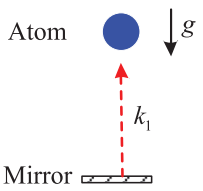

FIG. 2. A simplified model of Fig. 1 For atom gravimeters measuring g. Here, the control light $\vec{k}_1$ is upward oriented.

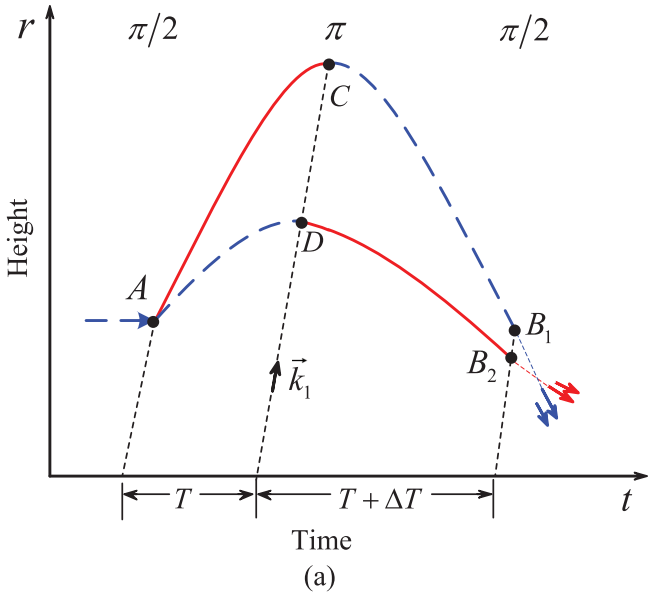

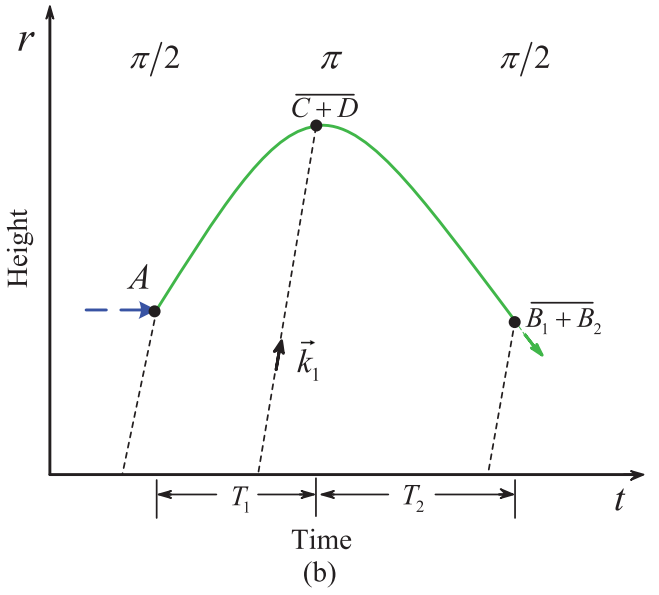

FIG. 3. The space-time diagram of a light-pulse atom interferometer (a) before and (b) after the average-path treatment.

can simplify the model of atom gravimeters to the control light tracking the atoms, which is described by Fig. 2. When the $\vec{k}_1$ beam interacts with the atoms, the states of the atoms change, which is shown in Fig. 3(a) (the interactions between the laser and atoms are reflected by points A, C, D, B_1, B_2), in which the horizontal axis and the vertical axis represent time and displacement, respectively. A detailed description of the space-time diagram can be found in [20,21]. Here, we consider that the timing of the third pulse has been artificially controlled to produce a time delay of ΔT, making the two pulse separations T and $T + \Delta T$, respectively. This pulse time delay is just adjusted at some point close to the location of the phase-locked photodiode. Because of the FSL, the pulses also take a certain amount of time to propagate to the actual location of the moving atom, which is the FSL time delay. We denote the FSL time delays of two pulse separations by δT_1 and δT_2.

Since the two moving paths for atoms are very close to each other, we can ignore the recoiling effect and regard the atoms as moving along the average path. Then, the space-time diagram in Fig. 3(a) can be simplified with the average-path method as in Fig. 3(b). Here, pulse separations T_1 and T_2 can be written as

$$T_1 = T + \delta T_1, \quad T_2 = T + \Delta T + \delta T_2. \tag{2}$$

Assuming that $\vec{r}(0) = 0$ and $\vec{v}_0$ respectively represent the initial displacement and velocity of the atom, we can derive the trajectory of the atom as $\vec{r}(t) = \vec{v}_0 t + \vec{g}t^2/2$. Therefore, the FSL time delays can be written as

$$\delta T_1 = \frac{\vec{r}(T)\cdot\vec{e}_c}{c} = \frac{\left(\vec{v}_0 T + \frac{1}{2}\vec{g}T^2\right)\cdot\vec{e}_c}{c}, \tag{3}$$

with c being the speed of light and

$$\delta T_2 = \frac{\vec{r}(2T+\Delta T)\cdot\vec{e}_c}{c} - \delta T_1 \approx \frac{\left(\vec{v}_0 T + \frac{3}{2}\vec{g}T^2\right)\cdot\vec{e}_c}{c}. \tag{4}$$

Here, we have kept the expression to the term of $1/c$ and omitted the small coupling term between ΔT and $1/c$. In the following, we analyze the FSL effect and pulse time-delay effect in the average-path method, where the total interference phase is approximately contributed by the three Raman light pulses and the mass-difference effect of atoms.

III. PULSE TIME-DELAY EFFECT AND FSL EFFECT IN ATOM GRAVIMETERS WITH THE CONTINUOUS CHIRP OF RAMAN PULSES

In this section, we calculate the phase shifts due to the pulse time delay and FSL in atom gravimeters and focus on making clear what causes the FSL effect and explaining the interesting phenomenon that although the pulse time delay is adjusted to about several thousand times the FSL time delay, the FSL effect introduces a significant bias in the g measurement, while the pulse time delay contributes a negligible effect.

To derive the contribution of the pulse time delay and the FSL effect in atom gravimeters, we should calculate the final interference phase shift after the two pulse separations, which is approximately contributed by the three Raman light pulses and the mass-difference effect of atoms. As the Doppler shift is produced by the atom moving, frequency chirps are usually applied to Raman lasers to compensate the Doppler shift. Thus, the effects related to the frequency chirps should also be taken into account.

First, we consider the phase of the effective Raman light field with the frequently used continuous chirps of the Raman pulses. We define t_r as the reference point of frequency chirps, ω_{10} (ω_{20}) as the frequency of the $\vec{k}_1$ ($\vec{k}_2$) light at $t = t_r$, and α_1 (α_2) and $\vec{n}_1$ ($\vec{n}_2$) as the frequency chirp and propagating direction of Raman beam $\vec{k}_1$ ($\vec{k}_2$), respectively. In this paper, we choose the reference point of frequency chirps at the π pulse, i.e., $t_r = T_1 = T + \delta T_1$. The phases of the two Raman lights can be described as [20]

$$\begin{aligned}\Phi_1(t,\vec{r}) &\approx \vec{k}_1(t)\cdot\vec{r} - \int \omega_1(t)dt \\ &= \frac{\omega_{10} + \alpha_1(t-t_r)}{c}\vec{n}_1\cdot\vec{r} \\ &\quad - \left[\omega_{10}(t-t_r) + \frac{1}{2}\alpha_1(t-t_r)^2\right]\end{aligned} \tag{5}$$

and

$$\begin{aligned}\Phi_2(t,\vec{r}) &\approx \vec{k}_2(t)\cdot\vec{r} - \int \omega_2(t)dt \\ &= \frac{\omega_{20} + \alpha_2(t-t_r)}{c}\vec{n}_2\cdot\vec{r} \\ &\quad - \left[\omega_{20}(t-t_r) + \frac{1}{2}\alpha_2(t-t_r)^2\right],\end{aligned} \tag{6}$$

where we have ignored the initial phases and kept the expressions to the term of $1/c$. Therefore, the phase for the effective light field is

$$\begin{aligned}\varphi_{\text{laser}}(t,\vec{r}) &= \Phi_1(t,\vec{r}) - \Phi_2(t,\vec{r}) \\ &\approx \frac{\omega_{10}\vec{n}_1 - \omega_{20}\vec{n}_2 + (\alpha_1\vec{n}_1 - \alpha_2\vec{n}_2)(t-t_r)}{c}\cdot\vec{r} \\ &\quad - \left[(\omega_{10}-\omega_{20})(t-t_r) + \frac{1}{2}(\alpha_1-\alpha_2)(t-t_r)^2\right],\end{aligned} \tag{7}$$

with the effective wave vector

$$\begin{aligned}\vec{k}_{\text{eff}}(t) &\equiv \vec{k}_1(t) - \vec{k}_2(t) \\ &= \frac{\omega_{10}\vec{n}_1 - \omega_{20}\vec{n}_2 + (\alpha_1\vec{n}_1 - \alpha_2\vec{n}_2)(t-t_r)}{c}.\end{aligned} \tag{8}$$

Therefore, inserting Eqs. (2), (3), and (4) into Eq. (7), we can derive the phase shift introduced by three Raman pulses as

$$\begin{aligned}\Delta\phi_{\text{laser}} &= 2\varphi_{\text{laser}}[T_1,\vec{r}(T_1)] - \varphi_{\text{laser}}[0,\vec{r}(0)] - \varphi_{\text{laser}}[T_2+T_1,\vec{r}(T_2+T_1)] \\ &\approx -\vec{k}_0\cdot\vec{g}T^2 + (\alpha_1-\alpha_2)T^2 - \vec{k}_0\cdot\vec{v}_\pi\Delta T - [\vec{k}_0\cdot\vec{g} - (\alpha_1-\alpha_2)]T\Delta T - \frac{1}{2}[\vec{k}_0\cdot\vec{g} - (\alpha_1-\alpha_2)]\Delta T^2 \\ &\quad - \vec{k}_0\cdot\vec{g}T^2\frac{3\vec{v}_\pi\cdot\vec{e}_c}{c} - (\alpha_1\vec{n}_1 - \alpha_2\vec{n}_2)T^2\cdot\frac{2\vec{v}_\pi}{c} + (\alpha_1-\alpha_2)T^2\frac{2\vec{v}_\pi\cdot\vec{e}_c}{c} \\ &\quad + (\omega_{10}-\omega_{20})\Delta T + \frac{\omega_{10}-\omega_{20}}{c}\vec{g}T^2\cdot\vec{e}_c,\end{aligned} \tag{9}$$

which has been kept to second order in ΔT and first order in $1/c$. Note that we also ignored the coupling term between ΔT and $1/c$ since it is so tiny. Here, $\vec{k}_0 = (\omega_{10}\vec{n}_1 - \omega_{20}\vec{n}_2)/c$ and $\vec{v}_\pi = \vec{v}_0 + \vec{g}(T + \delta T_1)$ represent the effective

wave vector and the velocity of atoms at the π pulse, respectively.

In nature, atoms in different states possess different internal-state energies, which contributes a mass-difference effect to the gravity measurement. Denoting the internal energy of the two hyperfine energy states for atoms by $\hbar\omega_e$ and $\hbar\omega_g$, we can write the mass-difference effect as

$$\Delta\phi_{\rm m} = -(\omega_e - \omega_g)\Delta T - \frac{\omega_e - \omega_g}{c}\vec{g}T^2 \cdot \vec{e}_c. \tag{10}$$

The detailed calculation can be found in our previous work (see Sec. III C 4 in [20]). When a detuning δ from the exact Raman resonance condition for the Raman pulse at the top of the atom fountain is considered, the following relation can be derived:

$$\omega_{10} - \omega_{20} = \omega_e - \omega_g + \delta + \vec{k}_0 \cdot \vec{v}_\pi. \tag{11}$$

Then, combining Eqs. (9), (10), and (11), we can approximately obtain the total interference phase shifts as

$$\begin{aligned}\Delta\Phi_{\rm total} &\approx \Delta\phi_{\rm laser} + \Delta\phi_{\rm m}\\ &\approx -\vec{k}_0 \cdot \vec{g}T^2 + (\alpha_1 - \alpha_2)T^2 - \vec{k}_0 \cdot \vec{v}_\pi \Delta T - [\vec{k}_0 \cdot \vec{g} - (\alpha_1 - \alpha_2)]T\Delta T - \frac{1}{2}[\vec{k}_0 \cdot \vec{g} - (\alpha_1 - \alpha_2)]\Delta T^2\\ &\quad - \vec{k}_0 \cdot \vec{g}T^2\frac{3\vec{v}_\pi \cdot \vec{e}_c}{c} - (\alpha_1\vec{n}_1 - \alpha_2\vec{n}_2)T^2 \cdot \frac{2\vec{v}_\pi}{c} + (\alpha_1 - \alpha_2)T^2\frac{2\vec{v}_\pi \cdot \vec{e}_c}{c} + \delta\Delta T + \delta\frac{\vec{g}T^2 \cdot \vec{e}_c}{c}\\ &\equiv -\vec{k}_0 \cdot \vec{g}_{\rm measured}T^2 + (\alpha_1 - \alpha_2)T^2.\end{aligned} \tag{12}$$

Further, the complete vectorial expression for the measured gravitational acceleration can be derived as

$$\begin{aligned}\vec{g}_{\rm measured} \cdot \vec{e}_k \approx \vec{g} \cdot \vec{e}_k\Bigg[1 &+ \frac{\vec{k}_0 \cdot \vec{g} - (\alpha_1 - \alpha_2)}{\vec{k}_0 \cdot \vec{g}}\frac{\Delta T}{T} + \frac{1}{2}\frac{\vec{k}_0 \cdot \vec{g} - (\alpha_1 - \alpha_2)}{\vec{k}_0 \cdot \vec{g}}\left(\frac{\Delta T}{T}\right)^2 - \frac{\delta}{\vec{k}_0 \cdot \vec{g}T^2}\Delta T\\ &+ \frac{2\vec{v}_\pi \cdot \vec{e}_c}{c} - \frac{\alpha_1 - \alpha_2}{\vec{k}_0 \cdot \vec{g}}\frac{2\vec{v}_\pi \cdot \vec{e}_c}{c} + \frac{\alpha_1\vec{n}_1 - \alpha_2\vec{n}_2}{\vec{k}_0 \cdot \vec{g}} \cdot \frac{2\vec{v}_\pi}{c} - \frac{\delta}{\vec{k}_0 \cdot \vec{g}T^2}\frac{\vec{g}T^2 \cdot \vec{e}_c}{c}\Bigg],\end{aligned} \tag{13}$$

with $\vec{e}_k = (\vec{n}_1 - \vec{n}_2)/|\vec{n}_1 - \vec{n}_2|$ being the direction of the effective wave vector.

For Eq. (13), the first-line corrective terms are related to the pulse time delay ΔT, and the second-line corrective terms belong to the FSL effect. Usually, the measured g is determined by finding the chirp rate at which a continuous chirp of the Raman frequency exactly cancels the gravity-induced Doppler shift, i.e., $\alpha_1 - \alpha_2 = \vec{k}_0 \cdot \vec{g}$. Therefore, the pulse time delay affects the gravity measurement mainly via the coupling term between the detuning δ and ΔT; however, the FSL effect influences the gravity measurement mainly through the corrective term related to $\alpha_1\vec{n}_1 - \alpha_2\vec{n}_2$ and the coupling term between the detuning δ and the FSL time delay (δT_1 and δT_2). In general, the detuning of the Raman pulse is extremely small since the resonance of the Raman pulse can be located accurately with the velocity preselection of atoms. Therefore, although the pulse time delay is about several thousand times the FSL time delay, the FSL effect introduces a significant bias in the g measurement, which is mainly contributed by the FSL corrective term related to $\alpha_1\vec{n}_1 - \alpha_2\vec{n}_2$, while the pulse time delay contributes a negligible effect $\delta\Delta T$. In addition, from Eq. (13), the δ-independent FSL correction can be eliminated by making the interferometer symmetric (the π Raman pulse is exactly at the top of the atomic fountain) to make $v_\pi = 0$, which is similar to the situation mentioned in [31], where the FSL correction cancels with other relativistic corrections when appropriate pulse times are used. The δ-dependent FSL correction can be compensated by appropriately adjusting the pulse times.

Based on the above analysis, one may want to make clear two questions: first, what is the FSL effect, and second, can the FSL time delay and the pulse time delay be regarded as quantitatively equivalent? Furthermore, how to experimentally verify the FSL effect and pulse time-delay effect is also extremely important to explore.

A. What is the FSL effect in atom gravimeters?

In this section, we discuss the physical origins of the FSL effect in atom gravimeters. Take the phase of the effective light field at the third Raman pulse, for example. According to Eq. (7), we can derive

$$\begin{aligned}\varphi_{\rm laser}[T_1 + T_2, \vec{r}(T_1 + T_2)] = &\left[\vec{k}_0 + \frac{(\alpha_1\vec{n}_1 - \alpha_2\vec{n}_2)T}{c}\right] \cdot \left\{\vec{v}_\pi[T + \Delta T + (\delta T_2 - \delta T_1)] + \frac{1}{2}\vec{g}[T + \Delta T + (\delta T_2 - \delta T_1)]^2\right\}\\ &- \left\{(\omega_{10} - \omega_{20})[T + \Delta T + (\delta T_2 - \delta T_1)] + \frac{1}{2}(\alpha_1 - \alpha_2)[T + \Delta T + (\delta T_2 - \delta T_1)]^2\right\}.\end{aligned} \tag{14}$$

Based on Eq. (11), δ and $\vec{k}_0 \cdot \vec{v}_\pi$ can be separated from $\omega_{10} - \omega_{20}$. Then, comparing Eqs. (13) and (14), we can well understand the origins of relative FSL corrective terms in Eq. (13):

$$\begin{aligned}
&\frac{2\vec{v}_\pi \cdot \vec{e}_c}{c} \leftarrow \text{the coupling of } \vec{k}_0 \text{ and } (\vec{v}_\pi + \vec{g}T)(\delta T_2 - \delta T_1) \text{ and the coupling of } \vec{k}_0 \cdot \vec{v}_\pi \text{ and } \delta T_2 - \delta T_1,\\
&-\frac{\alpha_1 - \alpha_2}{\vec{k}_0 \cdot \vec{g}} \frac{2\vec{v}_\pi \cdot \vec{e}_c}{c} \leftarrow \text{the coupling of } \alpha_1 - \alpha_2 \text{ and } \delta T_2 - \delta T_1,\\
&\frac{\alpha_1 \vec{n}_1 - \alpha_2 \vec{n}_2}{\vec{k}_0 \cdot \vec{g}} \cdot \frac{2\vec{v}_\pi}{c} \leftarrow \text{the contribution of the changes in the Raman wave vector } \frac{(\alpha_1 \vec{n}_1 - \alpha_2 \vec{n}_2)T}{c},\\
&-\frac{\delta}{\vec{k}_0 \cdot \vec{g} T^2} \frac{\vec{g}T^2 \cdot \vec{e}_c}{c} \leftarrow \text{the coupling of } \delta \text{ and } \delta T_2 - \delta T_1,
\end{aligned} \tag{15}$$

From Eq. (15), the FSL effect in atom gravimeters is caused not only by the retardation effects (δT_1 and δT_2) due to the finite speed of light but also by the changes in the Raman wave vector $(\alpha_1 \vec{n}_1 - \alpha_2 \vec{n}_2)T/c$. Therefore, the FSL effect cannot be simply called the FSL time-delay effect. In fact, the changes in the Raman wave vector $(\alpha_1 \vec{n}_1 - \alpha_2 \vec{n}_2)T/c$ are somewhere close to the location of the phase-locked photodiode and will also take some time to propagate to the actual location of the atom because of the finite speed of light. However, this coupled delay effect is so tiny that it can be absolutely ignored.

In addition, from Eq. (15), we find the FSL time delay (δT_1 and δT_2) has the same influencing mechanism as the pulse time delay (ΔT) on the gravity measurement. Therefore, the FSL time delay and the pulse time delay can be regarded as quantitatively equivalent.

B. Characteristics of the FSL effect in atom gravimeters

In this section, we analyze the characteristics of the FSL effect in atom gravimeters. We analyzed the FSL effect in atom gravimeters in our previous work [20] with the special case $\delta = -\vec{k}_0 \cdot \vec{v}_\pi$ (Raman lights are resonant at the π pulse) and $\vec{e}_c = \vec{n}_1$ (the $\vec{k}_1$ light is the control light). According to Eq. (13), we obtain a more complete expression for the measured gravity acceleration including the FSL correction as

$$\begin{aligned}
(\vec{g}_{\text{measured}} \cdot \vec{e}_k)_{\text{FSL}} \approx \vec{g} \cdot \vec{e}_k \Bigg[1 + \frac{2\vec{v}_\pi \cdot \vec{e}_c}{c} - \frac{\alpha_1 - \alpha_2}{\vec{k}_0 \cdot \vec{g}} \frac{2\vec{v}_\pi \cdot \vec{e}_c}{c}\\
+ \frac{\alpha_1 \vec{n}_1 - \alpha_2 \vec{n}_2}{\vec{k}_0 \cdot \vec{g}} \cdot \frac{2\vec{v}_\pi}{c} - \frac{\delta}{\vec{k}_0 \cdot \vec{g}} \frac{\vec{g} \cdot \vec{e}_c}{c} \Bigg].
\end{aligned} \tag{16}$$

Based on Eq. (16), the FSL effect in atom gravimeters depends on the directions of not only the two Raman lights $\vec{n}_1$ and $\vec{n}_2$ but the control light $\vec{e}_c$. Combined with the experimental setup, the direction of the control light $\vec{e}_c$ is decided by the position configuration of the reflecting mirror (see the discussion in Sec. II), and the directions $\vec{n}_1$ and $\vec{n}_2$ of the two Raman lights are related to the orientation of the effective wave vector $\vec{k}_0$. Thus, one can modulate the propagating directions of the lights involved in the measurement process, which can be achieved by changing the experimental configuration.

With the condition $\alpha_1 - \alpha_2 = \vec{k}_0 \cdot \vec{g}$, Eq. (16) can be further simplified as

$$g_{\text{FSL}} \approx g \left[1 + \frac{\alpha_1 \vec{n}_1 - \alpha_2 \vec{n}_2}{\vec{k}_0 \cdot \vec{g}} \cdot \frac{2\vec{v}_\pi}{c} - \frac{\delta}{\vec{k}_0 \cdot \vec{g}} \frac{\vec{g} \cdot \vec{e}_c}{c} \right], \tag{17}$$

where $g_{\text{FSL}} \equiv (\vec{g}_{\text{measured}} \cdot \vec{e}_k)_{\text{FSL}}$ and $g \equiv \vec{g} \cdot \vec{e}_k$. In the following, we study the FSL effect with different experimental configurations, where we use the following conventions: the direction of v_π is upward, $\alpha_1 - \alpha_2 = \vec{k}_0 \cdot \vec{g}$, the symbol $\uparrow$ ($\downarrow$) denotes that the orientation of the effective wave vector $\vec{k}_0 = \vec{k}_1(T_1) - \vec{k}_2(T_1)$ is upward (downward), and "bottom" ("top") denotes the reflecting mirror is at the bottom (top) of the device.

1. *FSL effect in the configuration with the reflecting mirror at the bottom of the device*

In this section, we discuss the FSL effect in the configuration where the reflecting mirror is at the bottom of the device. As shown in Fig. 4, the direction $\vec{e}_c$ of the control light ($\vec{k}_1$) in

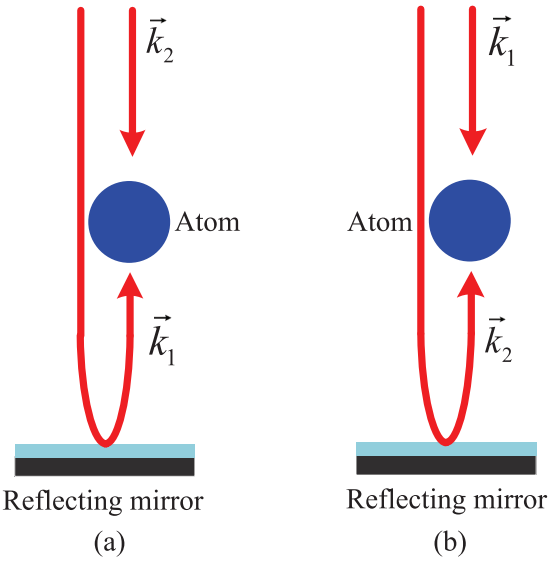

FIG. 4. Configurations for the reflecting mirror in an atom gravimeter being at the bottom of the device. The orientation of the effective wave vector $\vec{k}_0$ is upward in (a) and downward in (b).

this configuration is upward. Next, we consider the FSL effect with different orientations of the effective wave vector $\vec{k}_0$.

When the orientation of $\vec{k}_0$ is upward [see Fig. 4(a)], the gravitational acceleration including the FSL effect can be written as

$$(g_{\mathrm{FSL}})^{\uparrow}_{\mathrm{bottom}} \approx g\left[1+2\frac{v_\pi}{c}\left(\frac{\alpha_1+\alpha_2}{\alpha_1-\alpha_2}\right)_{\uparrow}+\frac{g\delta}{c(\alpha_1-\alpha_2)_{\uparrow}}\right]. \tag{18}$$

Similarly, when the orientation of $\vec{k}_0$ is downward [see Fig. 4(b)], the gravitational acceleration including the FSL effect can be written as

$$(g_{\mathrm{FSL}})^{\downarrow}_{\mathrm{bottom}} \approx g\left[1+2\frac{v_\pi}{c}\left(-\frac{\alpha_1+\alpha_2}{\alpha_1-\alpha_2}\right)_{\downarrow}+\frac{g\delta}{c(\alpha_1-\alpha_2)_{\downarrow}}\right]. \tag{19}$$

In the experiment measuring g with atom gravimeters, the signs of the frequency chirps applied to the two counterpropagating Raman lights in Figs. 4(a) and 4(b) are opposite since the orientations of $\vec{k}_{\mathrm{eff}}$ in the two cases are reversed. Therefore, we can derive the following relation:

$$(\alpha_1)_{\uparrow}=-(\alpha_1)_{\downarrow},\quad (\alpha_2)_{\uparrow}=-(\alpha_2)_{\downarrow}. \tag{20}$$

According to Eqs. (18), (19), and (20), with the two configurations of the effective wave vector $\vec{k}_0$, the FSL effect can be removed when calculating the averaged value $\bar{g}_{\mathrm{FSL}}=\frac{1}{2}[(g_{\mathrm{FSL}})^{\uparrow}_{\mathrm{bottom}}+(g_{\mathrm{FSL}})^{\downarrow}_{\mathrm{bottom}}]$. Alternatively, this effect can be obtained by calculating half the difference $(g_{\mathrm{FSL}})^{\uparrow}_{\mathrm{bottom}}-(g_{\mathrm{FSL}})^{\downarrow}_{\mathrm{bottom}}$.

2. *FSL effect in the configuration with the reflecting mirror at the top of the device*

Analogous to the analysis in last section, we discuss the FSL effect in the configuration where the reflecting mirror is at the top of the device in this section. As shown in Fig. 5, the direction $\vec{e}_c$ of the control light ($\vec{k}_2$) in this configuration is downward. Next, we also consider the FSL effect with different orientations of the effective wave vector $\vec{k}_0$.

When the orientation of $\vec{k}_0$ is upward [see Fig. 5(a)], the gravitational acceleration can be written as

$$(g_{\mathrm{FSL}})^{\uparrow}_{\mathrm{top}} \approx g\left[1+2\frac{v_\pi}{c}\left(\frac{\alpha_1+\alpha_2}{\alpha_1-\alpha_2}\right)_{\uparrow}-\frac{g\delta}{c(\alpha_1-\alpha_2)_{\uparrow}}\right]. \tag{21}$$

When the orientation of $\vec{k}_{\mathrm{eff}}$ is downward [see Fig. 5(b)], the gravitational acceleration can be written as

$$(g_{\mathrm{FSL}})^{\downarrow}_{\mathrm{top}} \approx g\left[1+2\frac{v_\pi}{c}\left(-\frac{\alpha_1+\alpha_2}{\alpha_1-\alpha_2}\right)_{\downarrow}-\frac{g\delta}{c(\alpha_1-\alpha_2)_{\downarrow}}\right]. \tag{22}$$

Similarly, the FSL effect can also be removed or obtained by performing a summation or difference between Eqs. (21) and (22).

3. *A simple discussion of the characteristics of the FSL effect in atom gravimeters*

Based on the analysis above, the FSL effect in atom gravimeters depends on the orientations of the control light and the effective wave vector, and each corrective term in Eq. (17) may be measured separately by making a differential measurement between different configurations: taking the difference between the measurement results of Figs. 4(a) and 5(a) or Figs. 4(b) and 5(b), one can derive the FSL correction related to the coupling between the detuning δ of the Raman pulse and the FSL time delay; performing a differential measurement between Figs. 4(a) and 5(b) or Figs. 4(b) and 5(a), one can obtain the FSL corrective term related to the changes in the effective wave vector (this term has been experimentally verified in [17]). Moreover, combining the configurations in Figs. 4(a) and 4(b) or Figs. 5(a) and 5(b), one can derive the total FSL correction.

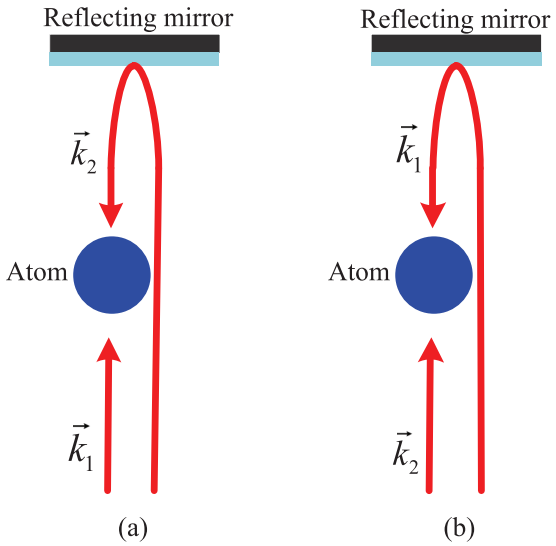

FIG. 5. Configurations of the reflecting mirror in an atom gravimeter being at the top of the device. The orientation of the effective wave vector $\vec{k}_0$ is upward in (a) and downward in (b).

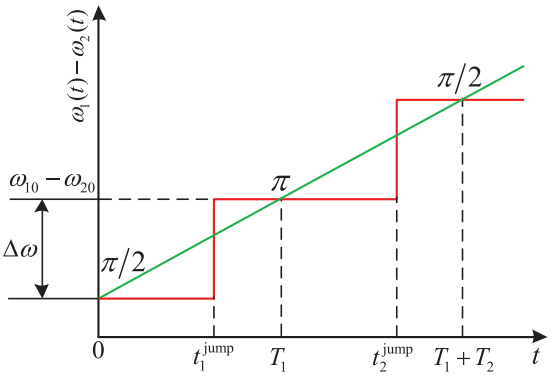

FIG. 6. Configuration of the frequency changes of the Raman pulses with the two frequency-chirp modes. Here, the green linear line represents the continuous-chirp mode, and the red folded line represents the stepped-chirp mode. t_1^{jump} and t_2^{jump} are the frequency-switching moments in the stepped-chirp mode. $\omega_{10}-\omega_{20}$ represents the frequency difference of two Raman beams at the π pulse, and $\Delta\omega$ is the difference between the frequency differences at any adjacent pulses.

IV. PULSE TIME-DELAY EFFECT AND FSL EFFECT IN ATOM GRAVIMETERS WITH THE STEPPED CHIRP OF RAMAN PULSES

In Sec. III, we discussed the pulse time-delay effect and the FSL effect in atom gravimeters with the continuous chirp of Raman pulses, where we focused on interpreting what the FSL effect is and proposing a possible experiment-verification scheme. As the pulse time-delay effect with this chirp mode affects the gravity measurement by the small coupling term $\delta\Delta T$, it is difficult to perform the related experimental verification. In this section, we mainly analyze the pulse time-delay effect and the FSL effect in atom gravimeters with the stepped chirp of Raman pulses, attempting to explore the scheme for testing the pulse time-delay effect.

Different from the continuous-chirp mode, in which the frequencies of Raman pulses linearly vary, the stepped frequency chirp switches the frequencies of Raman pulses between three fixed frequencies (see Fig. 6). Assuming the increments of the frequency and the wave vector for the effective light filed are $\Delta\omega$ and $\Delta\vec{k}$, respectively, we can write the phases of the effective light field at three pulses as

$$\begin{aligned}
\varphi_{\text{laser}}[0,\vec{r}(0)] &= 0,\\
\varphi_{\text{laser}}[T_1,\vec{r}(T_1)] &= \vec{k}_0\cdot\vec{r}(T_1) - (\omega_{10}-\omega_{20})\big(T_1 - t_1^{\text{jump}}\big) - (\omega_{10}-\omega_{20}-\Delta\omega)t_1^{\text{jump}},\\
\varphi_{\text{laser}}[T_1+T_2,\vec{r}(T_1+T_2)] &= (\vec{k}_0+\Delta\vec{k})\cdot\vec{r}(T_1+T_2) - (\omega_{10}-\omega_{20}+\Delta\omega)\big(T_1+T_2-t_2^{\text{jump}}\big) - (\omega_{10}-\omega_{20})\big(t_2^{\text{jump}}-T_1\big),
\end{aligned} \tag{23}$$

where we have chosen $(t=0,\vec{r}=\vec{0})$ as the origin. Then, we can derive the phase shift of the Raman pulses as

$$\begin{aligned}
\Delta\phi_{\text{laser}} &= 2\varphi_{\text{laser}}[T_1,\vec{r}(T_1)] - \varphi_{\text{laser}}[0,\vec{r}(0)] - \varphi_{\text{laser}}[T_1+T_2,\vec{r}(T_1+T_2)]\\
&\approx -\vec{k}_0\cdot\vec{g}T^2 - \vec{k}_0\cdot(\vec{v}_\pi+\vec{g}T)\Delta T - \frac{1}{2}\vec{k}_0\cdot\vec{g}\Delta T^2\\
&\quad - \vec{k}_0\cdot\vec{g}T^2\frac{3\vec{v}_\pi\cdot\vec{e}_c}{c} - \Delta\vec{k}\cdot 2\vec{v}_\pi T + \Delta\omega\big(T_1+T_2-t_2^{\text{jump}}+t_1^{\text{jump}}\big)+(\omega_{10}-\omega_{20})(\Delta T+\delta T_2-\delta T_1).
\end{aligned} \tag{24}$$

Combining Eqs. (10), (11), and (24), we can approximately obtain the total phase shift as

$$\begin{aligned}
\Delta\Phi_{\text{total}} &\approx \Delta\phi_{\text{laser}} + \Delta\phi_{\text{m}} \approx -\vec{k}_0\cdot\vec{g}T^2 - \vec{k}_0\cdot\vec{g}T\Delta T - \frac{1}{2}\vec{k}_0\cdot\vec{g}\Delta T^2 - \vec{k}_0\cdot\vec{g}T^2\frac{2\vec{v}_\pi\cdot\vec{e}_c}{c} - \Delta\vec{k}\cdot 2\vec{v}_\pi T\\
&\quad + \Delta\omega\big(T_1+T_2-t_2^{\text{jump}}+t_1^{\text{jump}}\big)+\delta\Delta T + \delta\frac{\vec{g}T^2\cdot\vec{e}_c}{c}.
\end{aligned} \tag{25}$$

If $\Delta\omega=(\alpha_1-\alpha_2)T$ and $\Delta\vec{k}=(\alpha_1\vec{e}_1-\alpha_2\vec{e}_2)T/c$, based on $\Delta\Phi_{\text{total}}\equiv-\vec{k}_0\cdot\vec{g}_{\text{measured}}T^2+(\alpha_1-\alpha_2)T^2$, the vectorial expression for the measured gravitational acceleration in the stepped-chirp mode can be derived as

$$\begin{aligned}
\vec{g}_{\text{measured}}\cdot\vec{e}_k \approx \vec{g}\cdot\vec{e}_k\Bigg[1 &- \frac{\alpha_1-\alpha_2}{\vec{k}_0\cdot\vec{g}}\frac{T-t_2^{\text{jump}}+t_1^{\text{jump}}}{T} + \frac{\vec{k}_0\cdot\vec{g}-(\alpha_1-\alpha_2)}{\vec{k}_0\cdot\vec{g}}\frac{\Delta T}{T} + \frac{1}{2}\left(\frac{\Delta T}{T}\right)^2 - \frac{\delta}{\vec{k}_0\cdot\vec{g}T^2}\Delta T\\
&+ \frac{2\vec{v}_\pi\cdot\vec{e}_c}{c} - \frac{\alpha_1-\alpha_2}{\vec{k}_0\cdot\vec{g}}\frac{2\vec{v}_\pi\cdot\vec{e}_c}{c} + \frac{\alpha_1\vec{n}_1-\alpha_2\vec{n}_2}{\vec{k}_0\cdot\vec{g}}\cdot\frac{2\vec{v}_\pi}{c} - \frac{\delta}{\vec{k}_0\cdot\vec{g}T^2}\frac{\vec{g}T^2\cdot\vec{e}_c}{c}\Bigg].
\end{aligned} \tag{26}$$

Through comparison, the pulse time-delay effect in the continuous-chirp mode mainly influences the g measurement via the small coupling term $\delta\Delta T$ [see Eq. (13)], while the situation is slightly different when the stepped-chirp mode is used. In this case, an additional quadratic correction [15,16] of ΔT enters except for the small coupling term. Therefore, one can modulate ΔT to verify the pulse time-delay effect experimentally.

V. SUMMARY

In this paper, we focused on studying the relationship between a time delay and the FSL effect. Based on the analysis, the FSL effect actually affects the gravity measurement in two ways: the time delay due to the FSL and the changes in the effective wave vector, in which the latter usually dominates. Furthermore, we found that the FSL time delay can be quantitatively regarded as equivalent to the pulse time delay since both of them actually affect the gravity measurement by changing the two pulse separations.

In addition, we discussed possible experimental schemes for verifying the FSL effect and the pulse time-delay effect. Based on the characteristics of the FSL effect in atom gravimeters, depending on the orientations of the lights in the measurement process, each FSL corrective term can be measured separately by making a differential or common mode measurement for different experimental configurations. The pulse time-delay effect can be experimentally verified with the stepped-frequency-chirp mode.

ACKNOWLEDGMENTS

We thank Dr. L. Floch for his thorough insights in editing our manuscript. This work is supported by the National Natural Science Foundation of China (Grant No. 91636221).

[1] K. Kuroda and N. Mio, Metrologia **28**, 75 (1991).
[2] V. D. Nagornyi, Y. M. Zanimonskiy, and Y. Y. Zanimonskiy, Metrologia **48**, 101 (2011).
[3] Ch. Rothleitner and O. Francis, Metrologia **48**, 187 (2011).
[4] V. D. Nagornyi, Y. M. Zanimonskiy, and Y. Y. Zanimonskiy, Metrologia **48**, 437 (2011).
[5] Ch. Rothleitner and O. Francis, Metrologia **48**, 442 (2011).
[6] V. D. Nagornyi, Metrologia **51**, 563 (2014).
[7] C. G. Shao, Y. J. Tan, J. Li, and Z. K. Hu, Metrologia **52**, 324 (2015).
[8] H. Baumann, F. Pythoud, D. Blas, S. Sibiryakov, A. Eichenberger, and E. E. Klingelé, Metrologia **52**, 635 (2015).
[9] H. Müller, S. W. Chiow, S. Herrmann, S. Chu, and K. Y. Chung, Phys. Rev. Lett. **100**, 031101 (2008).
[10] J. Le Gouët, T. E. Mehlstäubler, J. Kim, S. Merlet, A. Clairon, A. Landragin, and F. Pereira Dos Santos, Appl. Phys. B **92**, 133 (2008).
[11] Z. K. Hu, B. L. Sun, X. C. Duan, M. K. Zhou, L. L. Chen, S. Zhan, Q. Z. Zhang, and J. Luo, Phys. Rev. A **88**, 043610 (2013).
[12] S. Merlet, Q. Bodart, N. Malossi, A. Landragin, F. Pereira Dos Santos, O. Gitlein, and L. Timmen, Metrologia **47**, L9 (2010).
[13] M. K. Zhou, Z. K. Hu, X. C. Duan, B. L. Sun, L. L. Chen, Q. Z. Zhang, and J. Luo, Phys. Rev. A **86**, 043630 (2012).
[14] S. Zhan, X. C. Duan, M. K. Zhou, H. B. Yao, W. J. Xu, and Z. K. Hu, Opt. Lett. **40**, 29 (2015).
[15] A. Peters, Ph.D. thesis, Stanford University, 1998.
[16] A. Peters, K. Y. Chung, and S. Chu, Metrologia **38**, 25 (2001).
[17] B. Cheng, P. Gillot, S. Merlet, and F. Pereira Dos Santos, Phys. Rev. A **92**, 063617 (2015).
[18] S. Dimopoulos, P. W. Graham, J. M. Hogan, and M. A. Kasevich, Phys. Rev. Lett. **98**, 111102 (2007).
[19] S. Dimopoulos, P. W. Graham, J. M. Hogan, and M. A. Kasevich, Phys. Rev. D **78**, 042003 (2008).
[20] Y. J. Tan, C. G. Shao, and Z. K. Hu, Phys. Rev. A **94**, 013612 (2016).
[21] Y. J. Tan, C. G. Shao, and Z. K. Hu, Phys. Rev. D **95**, 024002 (2017).
[22] T. L. Gustavson, P. Bouyer, and M. A. Kasevich, Phys. Rev. Lett. **78**, 2046 (1997).
[23] A. Cronin, J. Schmiedmayer, and D. Pritchard, Rev. Mod. Phys. **81**, 1051 (2009).
[24] D. S. Durfee, Y. K. Shaham, and M. A. Kasevich, Phys. Rev. Lett. **97**, 240801 (2006).
[25] H. Müller, A. Peters, and S. Chu, Nature (London) **463**, 926 (2010).
[26] F. Sorrentino, Y.-H. Lien, G. Rosi, L. Cacciapuoti, M. Prevedelli, and G. M. Tino, New J. Phys **12**, 095009 (2010).
[27] M. A. Kasevich and S. Chu, Appl. Phys. B **54**, 321 (1992).
[28] Z. K. Hu, X. C. Duan, M. K. Zhou, B. L. Sun, J. B. Zhao, M. M. Huang, and J. Luo, Phys. Rev. A **84**, 013620 (2011).
[29] P. W. Graham, J. M. Hogan, M. A. Kasevich, and S. Rajendran, Phys. Rev. Lett. **110**, 171102 (2013).
[30] D. S. Weiss, B. C. Young, and S. Chu, Appl. Phys. B **59**, 217 (1994).
[31] S. Y. Lan, P. C. Kuan, B. Estey, D. English, J. M. Brown, M. A. Hohensee, and H. Müller, Science **339**, 554 (2013).